Appl. Math. Mech. -Engl. Ed., **38**(8), 1059–1070 (2017)
DOI 10.1007/s10483-017-2225-7
©Shanghai University and Springer-Verlag
Berlin Heidelberg 2017

Applied Mathematics and Mechanics (English Edition)

Thermal buckling analysis of functionally graded cylindrical shells*

Zeqing WAN[1,2], Shirong LI[1,2,†]

1. College of Civil Science and Engineering, Yangzhou University, Yangzhou 225127, Jiangsu Province, China;
2. College of Hydraulic Energy and Power Engineering, Yangzhou University, Yangzhou 225127, Jiangsu Province, China

Abstract Thermal buckling behavior of cylindrical shell made of functionally graded material (FGM) is studied. The material constituents are composed of ceramic and metal. The material properties across the shell thickness are assumed to be graded according to a simple power law distribution in terms of the volume fraction rule of mixtures. Based on the Donnell shell theory, a system of dimensionless partial differential equations of buckling in terms of displacement components is derived. The method of separation of variables is used to transform the governing equations to ordinary differential equations (ODEs). A shooting method is used to search for the numerical solutions of the differential equations under two types of boundary conditions. Effects of the power law index, the dimensionless geometrical parameters, and the temperature ratio on the critical buckling temperature are discussed in detail.

Key words functionally graded material (FGM), thermal buckling, cylindrical shell, shooting method

Chinese Library Classification O343.6
2010 Mathematics Subject Classification 35K55

1 Introduction

Circular cylindrical shell is a common structure in many engineering fields such as gun barrel, nuclear reactor, aerospace component, and heat supply pipeline. In many situations, these structures are used in extreme high temperature environments. Recent studies on new performance materials have addressed new materials known as functionally graded materials (FGMs), which have a smooth and continuous spatial variation of mechanical properties from one surface to the other. Typically, these materials consist of a mixture of ceramic and metal or a combination of different materials. They are high-performance heat-resistant materials which are able to withstand ultra high temperatures. With the increasing demand, FGMs have been widely used in general structures, especially in the thermal environments. Hence, the studies of the mechanical behavior of FGM structures, such as functionally graded beams, plates, and cylindrical shells under the thermal and mechanical loading have attracted more and more attention[1].

* Received Sept. 2, 2016 / Revised Dec. 22, 2016
Project supported by the National Natural Science Foundation of China (Nos. 11272278 and 11672260)
† Corresponding author, E-mail: srli@yzu.edu.cn

Eslami et al.[2] and Eslami and Javaheri[3] studied the thermal buckling behavior of perfect cylindrical shells made of homogeneous materials and cylindrical shells of composite materials based on the Donnell and improved Donnell equations. Reference [4] is the extension of the work of the authors to the thermal buckling analysis of imperfect cylindrical shells of isotropic materials.

Based on different classical and high-order shear deformation theory of shells, some comprehensive researches on the mechanical and thermal buckling behavior of FGM cylindrical shells have been reported[5–17]. Shahsiah and Eslami[5–6] investigated the thermal buckling behavior of functionally graded cylindrical shells and obtained the critical temperatures under three types of thermal loads with simply supported boundary conditions based on the Donnell and improved Donnell equations. Mirzavand et al.[7] studied the effect of imperfections on thermal buckling of simply supported FGM cylindrical shell by using the traditional Galerkin method. Based on the classical shell theory, Wu et al.[8] discussed the thermal buckling of functionally graded thin cylindrical shell under various thermal environments without considering the temperature-dependent material properties. Yaghoobi et al.[9] carried out a thermal buckling investigation on the axially functionally graded thin cylindrical shell.

Under the mechanical loading, lots of studies on the buckling of FGM cylindrical shells were performed. Li and Batra[10] studied the buckling of a simply supported three-layer circular cylindrical shell under axial compressive load, and Flugge's shell theory was used to study the buckling loads for different values of the geometric parameters and the variation in material parameters of the middle layer. By using the first-order shear deformation theory and the adjacent equilibrium criterion method, Khazaeinejad et al.[11] investigated the stability problem of an FGM circular cylindrical shell under combined external pressure and axial compression loads. Huang and Han[12] and Huang et al.[13] studied buckling of FGM cylindrical shells under axial compression and combined loads. Sun et al.[14] investigated the buckling of FGM cylindrical shells under combined thermal and compressive loads based on the classical Donnell shell theory, and the Galerkin method was adopted to discuss the imperfection sensitivity of an imperfect FGM cylindrical shell. An accurate buckling analysis for Reddy's high-order shear deformation FGM cylindrical shells under axial compression and thermal loads was presented by the same authors[15]. Sofiyev and Kuruoglu[16] investigated the buckling of FGM orthotropic cylindrical shells under external pressures using the shear deformation shell theory. The Galerkin method was used to solve the basic equations. Recently, some attention was attracted to elastoplastic FGMs. Buckling behavior of elastoplastic FGM cylindrical shells under combined axial compression and external pressure was investigated with classical shell theory by Zhang et al.[17]

In this paper, the thermal buckling behavior of cylindrical shells made of FGM is studied. The thermal loads are assumed to be uniform or transversely non-uniform temperature rise. A system of complicated coupling ordinary differential equations (ODEs) is established based on the Donnell shell theory by using the method of separation of variables. Then, two ends simply supported and two ends clamped boundary conditions are assumed, respectively. The shooting method is used to obtain numerical solutions of the two-point boundary value problem of the coupling ODEs. Comparative studies are presented for examination of the accuracy of the present analysis.

2 FGM properties

Consider a cylindrical shell made of FGM as shown in Fig. 1. Geometric parameters are defined as the length l, mid-surface radius R, and thickness h. We use cylindrical coordinates with the origin located at the mid-surface of the cylinder, and coordinates x, θ, and z in the axial, the circumferential, and the thickness directions, respectively.

The effective material properties, such as Young's modulus E, thermal expansion coefficient

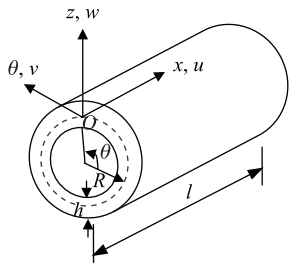

Fig. 1 Configuration and coordinate system of FGM cylindrical shell

α, and thermal conductivity K, are assumed changing[18] in the thickness direction z based on the following rule over the whole range of volume fraction:

$$P = P_{\mathrm{b}}\psi_{\mathrm{P}}(\eta), \tag{1}$$

where the subscript b refers to the homogenous material which is selected as the constituent at the inner surface of the FGM cylindrical shell. It is defined by

$$P_{\mathrm{b}} = P(-h/2). \tag{2}$$

In (1), $\psi_{\mathrm{P}}(\eta)$ is designed as a continuous dimensionless function of the coordinate z (or stepwise continuous function), which is expressed by

$$\psi_{\mathrm{P}} = 1 + (f_{\mathrm{P}} - 1)\Big(\frac{1}{2} + \eta\Big)^n, \quad -1/2 \leqslant \eta \leqslant 1/2, \tag{3}$$

where $f_{\mathrm{P}} = P_{\mathrm{t}}/P_{\mathrm{b}}$, $\eta = z/h$, n is a non-negative number, and the subscript t refers to the reference homogeneous material at the outer surface of the FGM cylindrical shell. Poisson's ratio ν of the shell is assumed to be constant since it usually varies very little in the thickness direction.

3 Fundamental equations

3.1 Geometrical relationships

Based on the Donnell shell theory, the normal and shear strains at a distance z from the shell middle surface are

$$\varepsilon_x = \varepsilon_x^0 + zk_x, \quad \varepsilon_\theta = \varepsilon_\theta^0 + zk_\theta, \quad \gamma_{x\theta} = \gamma_{x\theta}^0 + zk_{x\theta}, \tag{4}$$

where the strains of the mid-surface and the curvature defined in (4) are expressed as

$$(\varepsilon_x^0, \varepsilon_\theta^0, \gamma_{x\theta}^0) = \Big(u_{,x},\ \frac{1}{R}(v_{,\theta} + w),\ v_{,x} + \frac{1}{R}u_{,\theta}\Big), \tag{5}$$

$$(k_x, k_\theta, k_{x\theta}) = \Big(-w_{,xx},\ -\frac{1}{R^2}w_{,\theta\theta},\ -\frac{2}{R}w_{,x\theta}\Big), \tag{6}$$

where u, v, and w are the mid-surface displacements along the x-, θ-, and z-directions, respectively, and the subscript "," indicates a partial derivative.

3.2 Constitutive relations

The stress-strain relations are given by Hook's law as follows:

$$\begin{pmatrix} \sigma_x \\ \sigma_\theta \\ \tau_{x\theta} \end{pmatrix} = \frac{E}{1-\nu^2}\begin{pmatrix} 1 & \nu & 0 \\ \nu & 1 & 0 \\ 0 & 0 & \dfrac{1-\nu}{2} \end{pmatrix}\begin{pmatrix} \varepsilon_x \\ \varepsilon_\theta \\ \gamma_{x\theta} \end{pmatrix} - \frac{E\alpha T}{1-\nu}\begin{pmatrix} 1 \\ 1 \\ 0 \end{pmatrix}, \tag{7}$$

where σ_x, σ_θ, and $\tau_{x\theta}$ are the axial, circumferential, and shear stresses in the $Ox\theta$-plane, respectively, and T is the temperature rise with respect to the reference temperature. Here, we assume that the temperature rise varies only in the thickness direction. The value of T is defined as

$$T = T_{\rm b}\psi_{\rm T}(\eta), \tag{8}$$

where $T_{\rm b}$ denotes the temperature change at the inner surface of the shell, and $\psi_{\rm T}$ is a temperature variation function in the shell thickness direction.

The membrane forces and bending moments per unit length expressed in terms of the stress components through the thickness are

$$(N_x, N_\theta, N_{x\theta}) = \int_{-h/2}^{h/2} (\sigma_x, \sigma_\theta, \tau_{x\theta}){\rm d}z, \tag{9}$$

$$(M_x, M_\theta, M_{x\theta}) = \int_{-h/2}^{h/2} (\sigma_x, \sigma_\theta, \tau_{x\theta})z{\rm d}z. \tag{10}$$

Substituting (4) and (7) into (9) and (10) results in the following constitutive relation:

$$\begin{pmatrix} N_x \\ N_\theta \\ N_{x\theta} \\ M_x \\ M_\theta \\ M_{x\theta} \end{pmatrix} = \begin{pmatrix} A_{11} & A_{12} & 0 & B_{11} & B_{12} & 0 \\ A_{12} & A_{11} & 0 & B_{12} & B_{11} & 0 \\ 0 & 0 & Q_{11} & 0 & 0 & Q_{22} \\ B_{11} & B_{12} & 0 & D_{11} & D_{12} & 0 \\ B_{12} & B_{11} & 0 & D_{12} & D_{11} & 0 \\ 0 & 0 & Q_{22} & 0 & 0 & Q_{33} \end{pmatrix} \begin{pmatrix} \varepsilon_x^0 \\ \varepsilon_\theta^0 \\ \gamma_{x\theta}^0 \\ k_x \\ k_\theta \\ k_{x\theta} \end{pmatrix} - \begin{pmatrix} N_{\rm T} \\ N_{\rm T} \\ 0 \\ M_{\rm T} \\ M_{\rm T} \\ 0 \end{pmatrix}, \tag{11}$$

in which the stiffness coefficients are calculated by the following integrations:

$$\begin{cases} (A_{11}, B_{11}, D_{11}) = \displaystyle\int_{-h/2}^{h/2} (1, z, z^2)\frac{E}{1-\nu^2}{\rm d}z, \\ (A_{12}, B_{12}, D_{12}) = \displaystyle\int_{-h/2}^{h/2} (1, z, z^2)\frac{\nu E}{1-\nu^2}{\rm d}z, \\ (Q_{11}, Q_{22}, Q_{33}) = \displaystyle\int_{-h/2}^{h/2} (1, z, z^2)\frac{E}{2(1+\nu)}{\rm d}z. \end{cases} \tag{12}$$

The thermal axial force $N_{\rm T}$ and bending moment $M_{\rm T}$ are calculated by

$$(N_{\rm T}, M_{\rm T}) = \int_{-h/2}^{h/2} (1, z)\frac{E\alpha T}{1-\nu}{\rm d}z. \tag{13}$$

Substituting (1) into (12) yields the stiffness coefficients as follows:

$$\begin{cases} (A_{11}, A_{12}, Q_{11}) = \Big(1, \nu, \dfrac{1-\nu}{2}\Big)A\phi_1(\eta), \\ (B_{11}, B_{12}, Q_{22}) = \Big(1, \nu, \dfrac{1-\nu}{2}\Big)B\phi_2(\eta), \\ (D_{11}, D_{12}, Q_{33}) = \Big(1, \nu, \dfrac{1-\nu}{2}\Big)D\phi_3(\eta), \end{cases} \tag{14}$$

where A, B, and D are related to the reference homogeneous material shells, whose definitions are given by

$$A = \frac{E_{\rm b}h}{1-\nu^2}, \quad B = \frac{E_{\rm b}h^2}{1-\nu^2}, \quad D = \frac{E_{\rm b}h^3}{12(1-\nu^2)}, \tag{15}$$

and ϕ_i $(i=1,2,3)$ are dimensionless coefficients totally standing for the inhomogeneity of FGM cylindrical shell which are calculated by the following integrations:

$$\phi_1=\int_{-1/2}^{1/2}\psi_{\mathrm{E}}\mathrm{d}\eta,\quad \phi_2=\int_{-1/2}^{1/2}\psi_{\mathrm{E}}\eta\mathrm{d}\eta,\quad \phi_3=12\int_{-1/2}^{1/2}\psi_{\mathrm{E}}\eta^2\mathrm{d}\eta. \tag{16}$$

For a homogeneous cylindrical shell, $\phi_2=0$, and $\phi_1=\phi_3=f_{\mathrm{E}}$ when n=0, and $\phi_1=\phi_3=1$ when the value of n tends to infinity.

4 Governing equations

The nonlinear equilibrium equations of functionally graded cylindrical shell according to the Donnell theory are derived as follows[8]:

$$N_{x,x}+\frac{1}{R}N_{x\theta,\theta}=0, \tag{17}$$

$$\frac{1}{R}N_{\theta,\theta}+N_{x\theta,x}=0, \tag{18}$$

$$M_{x,xx}+\frac{2}{R}M_{x\theta,x\theta}+\frac{1}{R^2}M_{\theta,\theta\theta}-\frac{1}{R}N_\theta+N_x w_{,xx}+\frac{1}{R^2}N_\theta w_{,\theta\theta}+\frac{2}{R}N_{x\theta}w_{,x\theta}=0. \tag{19}$$

Once the buckling occurs immediately, the state variables can be assumed as the summations of the pre-buckling (denoted by subscript "0") and the incremental (denoted by subscript "1") deformations. Accordingly, the forces N_{ij} and the moments M_{ij} are divided into two terms representing the stable equilibrium and the neighboring state. Eliminating the pre-buckling equilibrium expressions and ignoring the nonlinear terms of the incremental variables, we obtain the governing equations for buckling as follows:

$$N_{x1,x}+\frac{1}{R}N_{x\theta1,\theta}=0, \tag{20}$$

$$\frac{1}{R}N_{\theta1,\theta}+N_{x\theta1,x}=0, \tag{21}$$

$$M_{x1,xx}+\frac{2}{R}M_{x\theta1,x\theta}+\frac{1}{R^2}M_{\theta1,\theta\theta}-\frac{1}{R}N_{\theta1}+N_{x0}w_{1,xx}+\frac{1}{R^2}N_{\theta0}w_{1,\theta\theta}+\frac{2}{R}N_{x\theta0}w_{1,x\theta}=0. \tag{22}$$

The forces and bending moments associated with the buckling state are

$$\begin{cases} N_{x1}=A_{11}u_{1,x}+\dfrac{A_{12}}{R}(v_{1,\theta}+w_1)-B_{11}w_{1,xx}-\dfrac{B_{12}}{R^2}w_{1,\theta\theta},\\ N_{\theta1}=A_{12}u_{1,x}+\dfrac{A_{11}}{R}(v_{1,\theta}+w_1)-B_{12}w_{1,xx}-\dfrac{B_{11}}{R^2}w_{1,\theta\theta},\\ N_{x\theta1}=Q_{11}\Big(v_{1,x}+\dfrac{1}{R}u_{1,\theta}\Big)-\dfrac{2Q_{22}}{R}w_{1,x\theta}, \end{cases} \tag{23}$$

$$\begin{cases} M_{x1}=B_{11}u_{1,x}+\dfrac{B_{12}}{R}(v_{1,\theta}+w_1)-D_{11}w_{1,xx}-\dfrac{D_{12}}{R^2}w_{1,\theta\theta},\\ M_{\theta1}=B_{12}u_{1,x}+\dfrac{B_{11}}{R}(v_{1,\theta}+w_1)-D_{12}w_{1,xx}-\dfrac{D_{11}}{R^2}w_{1,\theta\theta},\\ M_{x\theta1}=Q_{22}\Big(v_{1,x}+\dfrac{1}{R}u_{1,\theta}\Big)-\dfrac{2Q_{33}}{R}w_{1,x\theta}. \end{cases} \tag{24}$$

Substituting (23) and (24) into (20) to (22) and using (14), we get the stability equations in

terms of the displacement components as follows:

$$\phi_1 u_{1,xx} + \frac{1-\nu}{2R^2}\phi_1 u_{1,\theta\theta} + \frac{1+\nu}{2R}\phi_1 v_{1,x\theta} + \frac{\nu}{R}\phi_1 w_{1,x} - h\phi_2 w_{1,xxx} - \frac{h}{R^2}\phi_2 w_{1,x\theta\theta} = 0, \tag{25}$$

$$\frac{1+\nu}{2R}\phi_1 u_{1,x\theta} + \frac{1-\nu}{2}\phi_1 v_{1,xx} + \frac{1}{R^2}\phi_1 v_{1,\theta\theta} + \frac{1}{R^2}\phi_1 w_{1,\theta} - \frac{h}{R}\phi_2 w_{1,xx\theta} - \frac{h}{R^3}\phi_2 w_{1,\theta\theta\theta} = 0, \tag{26}$$

$$\begin{aligned}&\phi_2 u_{1,xxx} + \frac{\phi_2}{R^2}u_{1,x\theta\theta} + \frac{\phi_2}{R}v_{1,xx\theta} + \frac{\phi_2}{R^3}v_{1,\theta\theta\theta} + \frac{\nu}{R}\phi_2 w_{1,xx} + \frac{\phi_2}{R^3}w_{1,\theta\theta} - \frac{h}{12}\phi_3 w_{1,xxxx}\\ &- \frac{h}{6R^2}\phi_3 w_{1,xx\theta\theta} - \frac{h}{12R^4}\phi_3 w_{1,\theta\theta\theta\theta} - \Big(\frac{\nu}{Rh}\phi_1 u_{1,x} + \frac{1}{R^2h}\phi_1 v_{1,\theta} + \frac{1}{R^2h}\phi_1 w_1\\ &- \frac{\nu}{R}\phi_2 w_{1,xx} - \frac{\phi_2}{R^3}w_{1,\theta\theta}\Big) + \frac{1}{B}\Big(N_{x0}w_{1,xx} + \frac{1}{R^2}N_{\theta 0}w_{1,\theta\theta} + \frac{2}{R}N_{x\theta 0}w_{1,x\theta}\Big) = 0.\end{aligned} \tag{27}$$

5 Buckling analysis of FGM cylindrical shell

Considering that the pre-buckling deformation is axial-symmetric, we have the following initial membrane forces:

$$\begin{cases} N_{x0} = -N_{\mathrm{T}}, \\ N_{\theta 0} = N_{x\theta 0} = 0. \end{cases} \tag{28}$$

For convenience in the following analysis, we introduce the non-dimensional transformation as follows:

$$\begin{cases} (\xi, U, V, W) = \dfrac{1}{l}(x, u, v, w), \quad (\delta, \lambda) = \dfrac{1}{R}(h, l), \\ (n_x, n_\theta, n_{x\theta}, n_{\mathrm{T}}) = \dfrac{R^2}{D}(N_x, N_\theta, N_{x\theta}, N_{\mathrm{T}}), \\ (m_x, m_\theta, m_{x\theta}, m_{\mathrm{T}}) = \dfrac{R}{D}(M_x, M_\theta, M_{x\theta}, M_{\mathrm{T}}). \end{cases} \tag{29}$$

Thus, the thermal internal forces in dimensionless forms are as follows:

$$n_{\mathrm{T}} = \tau\beta_1, \quad m_{\mathrm{T}} = \tau\delta\beta_2, \tag{30}$$

in which

$$\begin{cases} \tau = \dfrac{12(1+\nu)\alpha_{\mathrm{b}}T_{\mathrm{b}}}{\delta^2}, \\ \beta_1(\eta) = \displaystyle\int_{-1/2}^{1/2} \psi_{\mathrm{E}}\psi_\alpha\psi_{\mathrm{T}}\mathrm{d}\eta, \\ \beta_2(\eta) = \displaystyle\int_{-1/2}^{1/2} \psi_{\mathrm{E}}\psi_\alpha\psi_{\mathrm{T}}\eta\mathrm{d}\eta, \end{cases} \tag{31}$$

where τ is used as the reference thermal load parameter. $\beta_i(\eta)$ $(i = 1, 2)$ are dimensionless coefficients.

By using the above non-dimensional quantities, the governing equations (25) to (27) can be

transformed into the dimensionless forms as follows:

$$\frac{\phi_1}{\lambda}\frac{\partial^2 U}{\partial\xi^2}+\frac{1-\nu}{2}\lambda\phi_1\frac{\partial^2 U}{\partial\theta^2}+\frac{1+\nu}{2}\phi_1\frac{\partial^2 V}{\partial\xi\partial\theta}+\nu\phi_1\frac{\partial W}{\partial\xi}-\frac{\delta\phi_2}{\lambda^2}\frac{\partial^3 W}{\partial\xi^3}-\delta\phi_2\frac{\partial^3 W}{\partial\xi\partial\theta^2}=0, \tag{32}$$

$$\frac{1+\nu}{2}\phi_1\frac{\partial^2 U}{\partial\xi\partial\theta}+\frac{1-\nu}{2}\frac{\phi_1}{\lambda}\frac{\partial^2 V}{\partial\xi^2}+\lambda\phi_1\frac{\partial^2 V}{\partial\theta^2}+\lambda\phi_1\frac{\partial W}{\partial\theta}-\frac{\delta\phi_2}{\lambda}\frac{\partial^3 W}{\partial\xi^2\partial\theta}-\delta\lambda\phi_2\frac{\partial^3 W}{\partial\theta^3}=0, \tag{33}$$

$$\begin{aligned}&\frac{\phi_2}{\lambda^2}\frac{\partial^3 U}{\partial\xi^3}+\phi_2\frac{\partial^3 U}{\partial\xi\partial\theta^2}+\frac{\phi_2}{\lambda}\frac{\partial^3 V}{\partial\xi^2\partial\theta}+\lambda\phi_2\frac{\partial^3 V}{\partial\theta^3}+\nu\frac{\phi_2}{\lambda}\frac{\partial^2 W}{\partial\xi^2}+\lambda\phi_2\frac{\partial^2 W}{\partial\theta^2}-\frac{\delta\phi_3}{12\lambda^3}\frac{\partial^4 W}{\partial\xi^4}\\&-\frac{\delta\phi_3}{6\lambda}\frac{\partial^4 W}{\partial\xi^2\partial\theta^2}-\frac{\lambda\delta\phi_3}{12}\frac{\partial^4 W}{\partial\theta^4}-\Big(\nu\frac{\phi_1}{\delta}\frac{\partial U}{\partial\xi}+\frac{\lambda\phi_1}{\delta}\frac{\partial V}{\partial\theta}+\frac{\lambda\phi_1}{\delta}W-\nu\frac{\phi_2}{\lambda}\frac{\partial^2 W}{\partial\xi^2}\\&-\lambda\phi_2\frac{\partial^2 W}{\partial\theta^2}\Big)-\frac{\delta}{12\lambda}\tau\beta_1\frac{\partial^2 W}{\partial\xi^2}=0,\end{aligned} \tag{34}$$

which consist of a system of complicated coupled partial differential equations with three unknown functions $U(\xi,\theta)$, $V(\xi,\theta)$, and $W(\xi,\theta)$.

To solve the system of (32) to (34), an effective method of separation of variables is adopted. We assume the displacement solutions in the form:

$$\begin{cases}U=\overline{U}(\xi)\cos(m\theta),\\V=\overline{V}(\xi)\sin(m\theta),\\W=\overline{W}(\xi)\cos(m\theta),\end{cases} \tag{35}$$

in which $0\leqslant\xi\leqslant 1$, $0\leqslant\theta\leqslant 2\pi$, and m indicates that the shell buckles in m half-wave in the θ-direction. Substitution of (35) into (32) to (34) gives the ODEs as follows:

$$\frac{\mathrm{d}^2\overline{U}}{\mathrm{d}\xi^2}-\frac{1-\nu}{2}m^2\lambda^2\overline{U}+\frac{1+\nu}{2}m\lambda\frac{\mathrm{d}\overline{V}}{\mathrm{d}\xi}-\frac{\delta\phi_2}{\lambda\phi_1}\frac{\mathrm{d}^3\overline{W}}{\mathrm{d}\xi^3}+\Big(\nu\lambda+m^2\frac{\delta\lambda\phi_2}{\phi_1}\Big)\frac{\mathrm{d}\overline{W}}{\mathrm{d}\xi}=0, \tag{36}$$

$$\frac{1+\nu}{2}m\lambda\frac{\mathrm{d}\overline{U}}{\mathrm{d}\xi}-\frac{1-\nu}{2}\frac{\mathrm{d}^2\overline{V}}{\mathrm{d}\xi^2}+m^2\lambda^2\overline{V}-m\frac{\delta\phi_2}{\phi_1}\frac{\mathrm{d}^2\overline{W}}{\mathrm{d}\xi^2}+\Big(m\lambda^2+m^3\frac{\delta\lambda^2\phi_2}{\phi_1}\Big)\overline{W}=0, \tag{37}$$

$$\begin{aligned}&\frac{\phi_2}{\lambda^2}\frac{\mathrm{d}^3\overline{U}}{\mathrm{d}\xi^3}-\Big(m^2\phi_2+\nu\frac{\phi_1}{\delta}\Big)\frac{\mathrm{d}\overline{U}}{\mathrm{d}\xi}+m\frac{\phi_2}{\lambda}\frac{\mathrm{d}^2\overline{V}}{d\xi^2}-\Big(m^3\lambda\phi_2+m\frac{\lambda\phi_1}{\delta}\Big)\overline{V}-\frac{\delta\phi_3}{12\lambda^3}\frac{\mathrm{d}^4\overline{W}}{\mathrm{d}\xi^4}\\&+\Big(\nu\frac{2\phi_2}{\lambda}+m^2\frac{\delta\phi_3}{6\lambda}-\frac{\delta}{12\lambda}\tau\beta_1\Big)\frac{\mathrm{d}^2\overline{W}}{\mathrm{d}\xi^2}-\Big(2m^2\lambda\phi_2+m^4\frac{\delta\lambda\phi_3}{12}+\frac{\lambda\phi_1}{\delta}\Big)\overline{W}=0.\end{aligned} \tag{38}$$

(36) to (38) are coupled ODEs including unknown functions of $\overline{U}(\xi)$, $\overline{V}(\xi)$, and $\overline{W}(\xi)$. For the convenience of solving the boundary value problem by the shooting method, (36) to (38) are rewritten as the following standard forms:

$$\frac{\mathrm{d}^2\overline{U}}{\mathrm{d}\xi^2}=a_{11}\overline{U}+a_{12}\frac{\mathrm{d}\overline{V}}{\mathrm{d}\xi}+a_{13}\frac{\mathrm{d}\overline{W}}{\mathrm{d}\xi}+a_{14}\frac{\mathrm{d}^3\overline{W}}{\mathrm{d}\xi^3}, \tag{39}$$

$$\frac{\mathrm{d}^2\overline{V}}{\mathrm{d}\xi^2}=a_{21}\frac{\mathrm{d}\overline{U}}{\mathrm{d}\xi}+a_{22}\overline{V}+a_{23}\overline{W}+a_{24}\frac{\mathrm{d}^2\overline{W}}{\mathrm{d}\xi^2}, \tag{40}$$

$$\frac{\mathrm{d}^4\overline{W}}{\mathrm{d}\xi^4}=c\Big(a_{31}\frac{\mathrm{d}\overline{U}}{\mathrm{d}\xi}+a_{32}\overline{V}+a_{33}\overline{W}+a_{34}\frac{\mathrm{d}^2\overline{W}}{\mathrm{d}\xi^2}\Big), \tag{41}$$

where $c=1/(\phi_3-12\phi_2^2/\phi_1)$, a_{ij} $(i=1,2,3;j=1,2,3,4)$ are coefficients listed in Appendix A.

So far, we finally arrive at a system of ODEs as (39) to (41). These equations and the corresponding boundary conditions constitute a two-point boundary value problem.

6 Temperature field distribution

We assume that the temperature rise of the FGM cylindrical shell changes from the inner surface to the outer one in the thickness direction. The value of T is found by solving the one-dimensional steady-state heat conduction equation

$$\frac{\mathrm{d}}{\mathrm{d}z}\Big(K(z)\frac{\mathrm{d}T(z)}{\mathrm{d}z}\Big)=0, \tag{42}$$

where $K(z)$ is the thermal conductivity. By integrating (42) and using the boundary conditions $T(h/2)=T_{\mathrm{t}}$ and $T(-h/2)=T_{\mathrm{b}}$, we assume that $T_{\mathrm{b}}\neq 0$ and write the expression of T in form of (8), in which ψ_{T} is given by

$$\psi_{\mathrm{T}}(\eta)=1+(f_{\mathrm{T}}-1)\frac{\displaystyle\int_{-1/2}^{\eta}1/K(\eta)\mathrm{d}\eta}{\displaystyle\int_{-1/2}^{1/2}1/K(\eta)\mathrm{d}\eta}, \tag{43}$$

where $f_{\mathrm{T}}=T_{\mathrm{t}}/T_{\mathrm{b}}$ is the ratio of the temperature rise at the outer and inner surfaces of the FGM cylindrical shell, and is the parameter to represent the inhomogeneity of the temperature field in the thickness direction. From (43), if $f_{\mathrm{T}}=1$, it follows that $\psi_{\mathrm{T}}=1$, which means that the temperature rise is uniform. Conversely, if $f_{\mathrm{T}}\neq 1$, the temperature field distribution is non-uniform.

7 Numerical results and discussion

In the numerical computation, the following two types of boundary conditions are considered. The first one is that the FGM cylindrical shell is immovably simply supported at the two ends (S-S). The boundary conditions are given by[5]

$$\overline{U}'=0,\quad \overline{V}=0,\quad \overline{W}=0,\quad \overline{W}''=0\quad \text{at}\quad \xi=0,1. \tag{44}$$

The second one is that the cylindrical shell is immovably clamped at the two ends (C-C). The boundary conditions in terms of the displacements can be written by

$$\overline{U}=0,\quad \overline{V}=0,\quad \overline{W}=0,\quad \overline{W}'=0\quad \text{at}\quad \xi=0,1. \tag{45}$$

The FGM cylindrical shell is assumed to be made of a ceramic (alumina) and a metal (steel) with pure metal and pure ceramic at the outer and inner surfaces, respectively. The material properties of the constituents are as follows:

$$\text{Steel}: E_{\mathrm{t}}=200\ \text{GPa},\quad \alpha_{\mathrm{t}}=11.7\times 10^{-6}\ (^{\circ}\text{C})^{-1},\quad K_{\mathrm{t}}=80\ \text{W}/(\text{m}\cdot\text{K}).$$
$$\text{Alumina}: E_{\mathrm{b}}=380\ \text{GPa},\quad \alpha_{\mathrm{b}}=7.4\times 10^{-6}\ (^{\circ}\text{C})^{-1},\quad K_{\mathrm{b}}=10.4\ \text{W}/(\text{m}\cdot\text{K}).$$

Poisson's ratio for both materials is chosen to be $\nu=0.3$.

To ensure the validity and accuracy of the present numerical method for buckling analysis of FGM cylindrical shell under thermal loads, some comparative studies are carried out. Assuming the length to radius ratio $\lambda=1$, and the power law index $n=0$ or n tends to infinity, the critical buckling temperature rise, ΔT_{cr}, of homogeneous cylindrical shell with two ends simply supported for different values of the thickness to radius ratio δ under uniform temperature rise is obtained in Table 1. An excellent agreement can be seen between the results of the present and those in the literature. In Table 1, $\Delta T_{\mathrm{cr}}=\tau\delta^2/(12(1+\nu)\alpha_{\mathrm{b}})$.

Table 1 Comparison of present values of critical temperature rise $\Delta T_{\rm cr}$ (°C) with those in literature for uniformly heated simply supported homogenous cylindrical shell

n		$\delta = 0.001$	$\delta = 0.005$	$\delta = 0.007\,5$	$\delta = 0.01$
0 (metal)	Present	36.21	181.06	271.61	363.22
	Ref. [2]	36.21	181.21	272.86	362.76
	Ref. [9]	36.23	181.19	271.79	362.39
10^6 (ceramic)	Present	57.25	286.26	429.41	574.26
	Ref. [2]	57.26	286.51	431.41	573.56
	Ref. [9]	57.29	286.48	429.73	572.90

First, we consider the case that the temperature rise is uniform. Namely, $f_{\rm T} = 1$. Figure 2 shows the continuous variation of the critical buckling temperature of the FGM shell under S-S and C-C end constraints with the thickness to radius ratio δ for some specified values of power law index n. As seen in this figure, the dimensionless critical buckling temperature decreases with an increase in the values of δ. Also, it is clear that for the shell with a larger value of power index n the critical buckling temperature is higher. This is due to that the shell has a larger amount of the ceramic components which leads to a stronger bending stiffness of it. Furthermore, Fig. 2 illustrates the critical buckling temperature of FGM cylindrical shell under the two types of boundary conditions for some specified values of power law index n. Critical buckling temperatures of the shell under C-C end constraints are higher than those of the shell under S-S end constraints because bending rigidity produced by C-C ends is stronger than that by S-S ends. However, with the increase of the thickness to radius ratio δ, the difference of the critical temperatures produced by the boundary conditions tends to be not obvious.

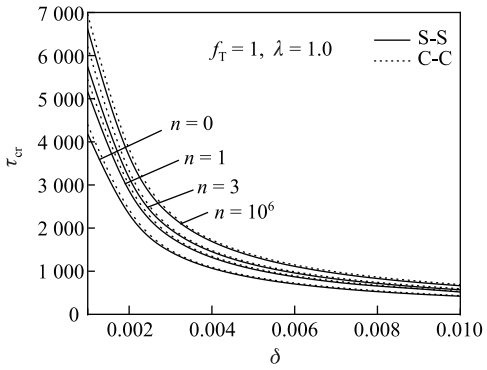

Fig. 2 Curves of dimensionless critical buckling temperature $\tau_{\rm cr}$ of FGM shell versus thickness to radius ratio δ for some specified values of n under uniform temperature rise

Next, for the case of transversely non-uniform temperature rise, the values of the dimensionless critical buckling temperature of the FGM cylindrical shell for different values of parameters of n and δ for some specified values of the temperature ratio $f_{\rm T}$ are listed in Table 2. For the fixed values of n and $f_{\rm T}$, the results in the first and the second rows correspond, respectively, to the S-S and C-C shells. The difference between the results of the two rows reveals the effect of the boundary constraints on the critical buckling temperature. It is observed that the critical buckling temperature increases with the increase in the power law index n and decreases along with the increase of the thickness to radius ratio δ. This is because the increase of n leads to the increase of both the extensional and the bending rigidities of the shell. It needs to notice that from the definition of the dimensionless thermal load parameter τ in (31), we can see that the actual critical buckling temperature $T_{\rm b}$ is proportional to the square of δ. Therefore, the actual critical buckling temperatures are higher for $\delta = 0.01$ than those for $\delta = 0.001$. From the table, we can also find that the non-dimensional critical buckling temperature for a given

Table 2 Dimensionless critical buckling temperature τ_{cr} varying with parameters of n and δ under transversely non-uniform temperature rise ($\lambda = 1.0$)

n	f_T		δ									
			0.001	0.002	0.003	0.004	0.005	0.006	0.007	0.008	0.009	0.010
0	3	a	2 090.16(7)	1 045.08(17)	696.78(7)	522.55(4)	418.04(4)	348.36(11)	298.84(1)	261.30(5)	232.25(2)	209.65(1)
		b	2 196.17(7)	1 094.35(2)	708.79(6)	534.48(4)	429.84(4)	359.25(5)	309.51(6)	271.41(6)	240.35(7)	218.05(7)
	5	a	1 393.44(7)	696.72(17)	464.52(7)	348.37(4)	278.69(4)	232.24(11)	199.14(1)	176.46(1)	154.84(2)	139.77(1)
		b	1 464.45(7)	729.56(2)	471.96(6)	356.34(3)	286.54(4)	239.34(5)	206.34(6)	180.94(6)	160.23(7)	144.19(7)
	9	a	836.06(7)	418.07(11)	278.71(7)	209.02(4)	167.21(4)	139.36(6)	119.49(1)	104.52(5)	92.90(2)	83.86(1)
		b	878.47(9)	437.74(2)	283.69(6)	213.79(3)	171.92(4)	144.35(4)	123.80(6)	108.74(6)	97.61(7)	87.48(7)
3	3	a	2 468.17(1)	1 233.21(5)	822.95(1)	616.63(5)	493.29(5)	413.22(1)	352.35(2)	310.66(1)	274.09(4)	246.84(1)
		b	2 690.83(4)	1 287.25(5)	836.08(6)	629.70(5)	506.18(5)	422.95(5)	366.07(3)	319.66(6)	286.94(4)	259.40(5)
	5	a	1 576.34(1)	787.61(5)	525.10(9)	393.82(5)	315.05(5)	263.91(1)	225.03(2)	198.41(1)	175.05(4)	157.65(1)
		b	1 719.07(3)	822.06(6)	533.65(7)	402.17(5)	324.03(5)	270.12(6)	233.80(3)	205.93(6)	184.52(4)	165.67(5)
	9	a	923.42(1)	460.53(1)	304.82(9)	228.61(5)	182.88(5)	153.20(1)	130.63(2)	115.18(1)	101.62(4)	91.51(1)
		b	997.92(4)	477.20(5)	309.78(7)	233.46(5)	187.66(5)	156.81(5)	135.72(3)	118.67(5)	106.38(4)	96.17(5)
10^6	3	a	3 304.34(7)	1 652.26(1)	1 101.54(7)	826.10(4)	660.88(4)	550.73(11)	472.24(1)	413.09(5)	367.17(2)	331.44(1)
		b	3 473.27(6)	1 730.05(2)	1 118.79(8)	844.96(4)	679.48(4)	567.57(6)	489.30(6)	430.55(4)	383.11(6)	344.71(6)
	5	a	2 202.86(7)	1 101.52(11)	734.35(7)	550.73(4)	440.58(4)	367.18(6)	314.82(1)	275.39(5)	244.78(2)	220.96(1)
		b	2 314.58(9)	1 153.35(2)	745.99(7)	563.32(3)	452.98(4)	378.62(6)	326.19(6)	286.50(5)	257.20(6)	229.81(6)
	9	a	1 321.70(7)	660.85(17)	441.22(17)	330.43(4)	264.34(4)	221.78(12)	188.89(1)	167.38(1)	146.86(2)	132.57(1)
		b	1 388.73(9)	692.00(2)	448.20(6)	337.99(3)	271.78(4)	228.19(4)	195.71(6)	171.90(5)	154.32(6)	137.88(6)

Note: numbers in brackets are circumferential half-wave numbers of buckling modes
[a]S-S; [b]C-C

value of n decrease with an increase in f_T, which is due to the fact that the increase in the value of f_T results in the increase of the non-uniform degree of the temperature fields.

Finally, we investigate the effect of the variation of the length to radius ratio on the critical buckling temperature. For some specified values of n, dimensionless critical buckling temperatures τ_{cr} as a function of the length to radius ratio λ for both uniformly ($f_T = 1$) and non-uniformly ($f_T = 3$) heated FGM cylindrical shells with S-S ends are shown in Fig. 3 and Fig. 4, respectively. From these two figures, it can be found that the critical buckling temperature is almost constant for different values of λ. Hence, the value of the length to radius ratio λ has no effect on the critical buckling temperature of the shell.

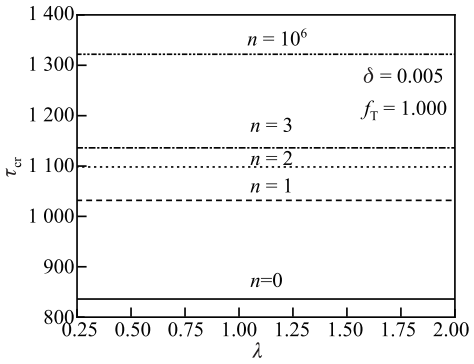

Fig. 3 Dimensionless critical buckling temperature of shell under uniform temperature rise versus parameter λ for some specified values of n

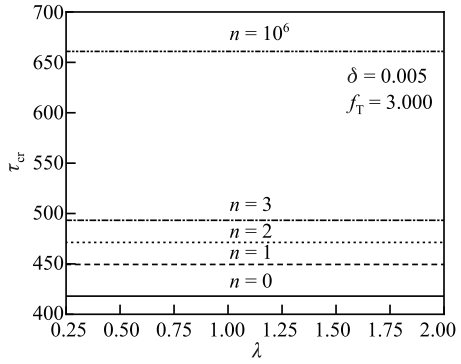

Fig. 4 Dimensionless critical buckling temperature of shell under non-uniform temperature rise versus parameter λ for some specified values of n

8 Conclusions

Based on the classical Donnell shell theory, the thermal buckling responses of an FGM cylindrical shell have been analyzed by solving the system of dimensionless partial differential governing equations for buckling in terms of the displacement components. The material properties are assumed to vary in the thickness direction according to a power law function of the radial coordinate except that Poisson's ratio is assumed to be a constant. Method of separation of variables is used to transform the governing equations into ODEs with three coupled unknown functions. Then, considering the S-S and C-C ends, a buckling analysis of functionally graded shell under uniform and transversely non-uniform thermal loads is carried out by using the shooting method. The following conclusions are drawn from the numerical results.

(i) The values of critical buckling temperature for the functionally graded cylindrical shell with S-S ends are generally smaller than the corresponding values for the C-C cylindrical shell.

(ii) The dimensionless critical buckling temperature for the two types of thermal loads decreases with the increase of the thickness to radius ratio δ. Regarding to the simply supported shell, the increase in the length to radius ratio λ has no effect on the buckling temperature.

(iii) The dimensionless critical buckling temperature increases along with the increase of the power law index n because the increment of the ceramic constituent can produce more stiffness in the FGM cylindrical shell structure.

(iv) The value of the ratio of the outer and inner surface temperature rise of the shell, f_{T}, has obvious effects on the inhomogeneity of the temperature fields. The non-dimensional critical buckling temperature decreases with the increase of f_{T}.

References

[1] Gupta, A. and Talha, M. Recent development in modeling and analysis of functionally graded materials and structures. *Progress in Aerospace Sciences*, **79**, 1–14 (2015)

[2] Eslami, M. R., Ziaii, A. R., and Ghorbanpour, A. Thermoelastic buckling of thin cylindrical shells based on improved stability equations. *Journal of Thermal Stresses*, **19**(4), 299–315 (1996)

[3] Eslami, M. R. and Javaheri, R. Buckling of composite cylindrical shells under mechanical and thermal loads. *Journal of Thermal Stresses*, **22**(6), 527–545 (1999)

[4] Eslami, M. R. and Shahsiah, R. Thermal buckling of imperfect cylindrical shells. *Journal of Thermal Stresses*, **24**(1), 71–89 (2001)

[5] Shahsiah, R. and Eslami, M. R. Thermal buckling of functionally graded cylindrical shell. *Journal of Thermal Stress*, **26**(3), 277–294 (2003)

[6] Shahsiah, R. and Eslami, M. R. Functionally graded cylindrical shell thermal instability based on improved Donnell equations. *AIAA Journal*, **41**(41), 1819–1826 (2012)

[7] Mirzavand, B., Eslami, M. R., and Shahsiah, R. Effect of imperfections on thermal buckling of functionally graded shells. *AIAA Journal*, **43**(43), 2073–2076 (2015)

[8] Wu, L. H., Jiang, Z. Q., and Liu, J. Thermoelastic stability of functionally graded cylindrical shells. *Composite Structures*, **70**(1), 60–68 (2005)

[9] Yaghoobi, H., Fereidoon, A., and Shahsiah, R. Thermal buckling of axially functionally graded thin cylindrical shell. *Journal of Thermal Stresses*, **34**(12), 1250–1270 (2011)

[10] Li, S. R. and Batra, R. C. Buckling of axially compressed thin cylindrical shells with functionally graded middle layer. *Thin-Walled Structures*, **44**(10), 1039–1047 (2006)

[11] Khazaeinejad, P., Najafizadeh, M. M., Jenabi, J., and Isvandzibaei, M. R. On the buckling of functionally graded cylindrical shells under combined external pressure and axial compression. *Journal of Pressure Vessel Technology*, **132**(6), 1–6 (2010)

[12] Huang, H. W. and Han, Q. Buckling of imperfect functionally graded cylindrical shells under axial compression. *European Journal of Mechanics A/Solids*, **27**(6), 1026–1036 (2008)

[13] Huang, H. W., Han, Q., Feng, N. W., and Fan, X. J. Buckling of functionally graded cylindrical shells under combined loads. *Mechanics of Advanced Materials and Structures*, **18**(5), 337–346 (2011)

[14] Sun, J. B., Xu, X. S., and Lim, C. M. Buckling of functionally graded cylindrical shells under combined thermal and compressive loads. *Journal of Thermal Stresses*, **37**(3), 340–362 (2014)

[15] Sun, J. B., Xu, X. S., Lim, C. W., and Qiao, W. Y. Accurate buckling analysis for shear deformable FGM cylindrical shells under axial compression and thermal loads. *Composite Structures*, **123**(5), 246–256 (2015)

[16] Sofiyev, A. H. and Kuruoglu, N. Buckling and vibration of shear deformable functionally graded orthotropic cylindrical shells under external pressures. *Thin-Walled Structures*, **78**(78), 121–130 (2014)

[17] Zhang, Y. Q., Huang, H. W., and Han, Q. Buckling of elastoplastic functionally graded cylindrical shells under combined compression and pressure. *Composites*: *Part B*, **69**(69), 120–126 (2015)

[18] Li, S. R., Wan, Z. Q., and Wang, X. Homogenized and classical expressions for static bending solutions for functionally graded material Levinson beams. *Applied Mathematics and Mechanics* (*English Edition*), **36**(7), 895–910 (2015) DOI 10.1007/s10483-015-1956-9

Appendix A

Expressions for coefficients in (39) to (41) are

$$
\begin{aligned}
&a_{11}=\frac{1-\nu}{2}m^2\lambda^2,\quad a_{12}=-\frac{1+\nu}{2}m\lambda,\quad a_{13}=-\nu\lambda-m^2\frac{\delta\lambda\phi_2}{\phi_1},\quad a_{14}=\frac{\delta\phi_2}{\lambda\phi_1},\\
&a_{21}=\frac{1+\nu}{1-\nu}m\lambda,\quad a_{22}=\frac{2m^2\lambda^2}{1-\nu},\quad a_{23}=\frac{2m\lambda^2}{1-\nu}+\frac{2m^3}{1-\nu}\frac{\delta\lambda^2\phi_2}{\phi_1},\quad a_{24}=-\frac{2m}{1-\nu}\frac{\delta\phi_2}{\phi_1},\\
&a_{31}=-\nu\frac{12\lambda^3\phi_1}{\delta^2},\quad a_{32}=-\frac{12m\lambda^4\phi_1}{\delta^2},\\
&a_{33}=-\Big(\frac{12\lambda^4\phi_1}{\delta^2}+\frac{12m^2\lambda^4\phi_2}{\delta}-\frac{12m^4\lambda^4\phi_2^2}{\phi_1}+m^4\lambda^4\phi_3\Big),\\
&a_{34}=\nu\frac{12\lambda^2\phi_2}{\delta}-\frac{24m^2\lambda^2\phi_2^2}{\phi_1}+2m^2\lambda^2\phi_3-\lambda^2\tau\beta_1.
\end{aligned}
$$